JOURNAL OF SPACECRAFT AND ROCKETS
Vol. 42, No. 3, May–June 2005

Aerodynamic Safing Approach for the 2001 Mars Odyssey Spacecraft During Aerobraking

Jim D. Chapel,* Mark A. Johnson,† Wayne P. Sidney,‡ William H. Willcockson,‡ and Douglas Gulick§
Lockheed Martin Space Systems, Denver, Colorado 80201
and
Jason A. Wynn†
Advanced Solutions, Inc., Littleton, Colorado 80127

The 2001 Mars Odyssey spacecraft represents the third generation of aerobraking designs, following Magellan's pioneering aerobraking demonstration at Venus and Mars Global Surveyor's planned operational aerobraking at Mars. Aerobraking provides significant advantages for interplanetary spacecraft by reducing the size of the required propulsion system and propellant load, thereby allowing larger payloads for the same launch mass. However, aerobraking is not without risk; relatively small command errors or brief inattention to the highly variable atmospheric dynamics can lead to disaster. This paper describes how the 2001 Mars Odyssey aerobraking design and operations managed the inherent aerodynamics-related risks of aerobraking. We describe the configuration changes Odyssey used during aerobraking orbits and how the operations team managed those configurations. We present a detailed vehicle dynamics model derived for Odyssey's aerobraking safe-mode configuration, as well as the predicted attitude response during aerobraking safing events. Contingency procedures were developed before aerobraking and included an option to "pop-up" out of the atmosphere if aerobraking operations began to endanger spacecraft health and safety. We describe the criteria and decision-making process for commanding pop-up maneuvers. Finally, flight results from Odyssey's aerobraking experience are presented including an assessment of the aerodynamic safing approach in response to the highly variable atmospheric conditions.

Nomenclature

C_{MX} = moment coefficient about X axis
C_{MZ} = moment coefficient about Z axis
θ = Euler rotation angle (pitch)
ϕ = Euler rotation angle (yaw)

Introduction

THE 2001 Mars Odyssey spacecraft's science mission consists of performing Mars observations from a 400-km nearly circular polar orbit.[1] To save launch vehicle cost, the use of aerobraking was baselined to lighten the vehicle and greatly reduce the propellant required for Mars orbit insertion (MOI). The Mars Odyssey aerobraking approach relied heavily on previous design and flight operations experience from Magellan's pioneering aerobraking demonstration at Venus[2] and Mars Global Surveyor's (MGS) aerobraking experience at Mars.[3] Odyssey's aerobraking approach was also based upon that of the ill-fated Mars Climate Orbiter, which never proved its aerobraking design because of failure to achieve Mars orbit.[4,5]

The Odyssey aerobraking strategy employed a propulsive capture into a large parking orbit, followed by aerobraking maneuvers to gradually circularize the orbit over several hundred orbits. Each aerobraking orbit used a low-energy drag pass through the upper atmosphere, thereby slightly reducing the orbital energy of the spacecraft every pass. Over a period spanning slightly less than three months, the initial 18.5-h orbit achieved by Odyssey's MOI burn was reduced to less than 2 h.

Several aspects of the Odyssey aerobraking experience distinguish it from the Magellan and MGS experiences previously reported in the literature. Whereas the Magellan aerobraking was experimental and performed only after the primary science mission had been completed, both the MGS and the Odyssey spacecraft missions required that aerobraking be successfully performed before their primary science missions could begin. They were both designed and analyzed to support aerobraking, including uncertainties and off-nominal conditions. Early in its mission, MGS suffered an anomaly that significantly reduced the maximum allowable aerobraking dynamic pressure, and therefore the drag passes were flown at higher, less efficient, altitudes. The MGS design also allowed for trimming of the aerodynamics in flight by using gimbal-driven appendages. Because Odyssey's aerobraking configuration did not have any ability to trim the aerodynamics in flight, and because Odyssey's aerobraking drag passes reached altitudes as low as 90 km above the Mars surface, the aerodynamic prediction accuracy was crucial. Odyssey's lower altitudes and relatively aggressive aerobraking profile presented new challenges to ensure the aerodynamic safety of the spacecraft. This paper presents several innovations to ensure the aerodynamic safety of aerobraking spacecraft. Specifically, contributions include application of high-fidelity modeling and analysis techniques to assess aerodynamic safety of various Mars aerobraking configurations and attitude profiles, design and implementation of autonomous sequence adjustments to account for Mars atmospheric variability, refinements of monitoring and decision criteria for safing maneuvers, and an assessment of these approaches with use of in-flight data from aerobraking altitudes never previously attempted.

Odyssey Configuration for Aerobraking

Before each drag pass, the Odyssey spacecraft was placed into the aerodynamically stable, high-drag configuration shown in Fig. 1. This configuration approximately aligned the vehicle's $-Y$ axis with the local velocity vector and the $-Z$ axis the nadir vector. Using an onboard orbital ephemeris developed from ground navigation solutions, Odyssey maintained this attitude through each drag pass. Because each drag pass changed the orbit geometry, frequent orbital ephemeris updates were required. For the drag pass itself, the attitude control system was reconfigured from reaction-wheel control to thruster-based control. Because of the statically stable aerobraking

Received 21 January 2003; accepted for publication 4 November 2004.

*Senior Staff Engineer. Senior Member AIAA.
†Staff Engineer.
‡Senior Staff Engineer.
§Staff Engineer. Senior Member AIAA.

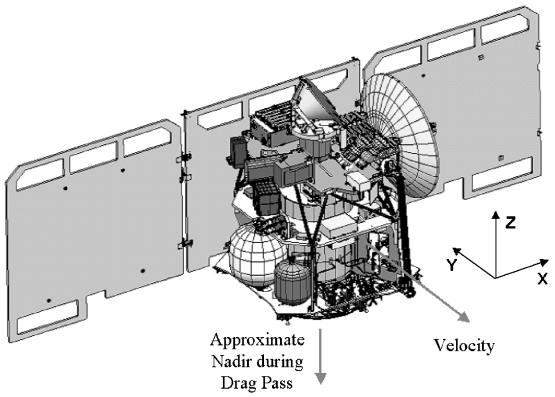

Fig. 1 2001 Mars Odyssey in aerobraking configuration.

configuration, the controller was designed with large deadbands to minimize fuel consumption. The periapsis altitude, and hence the amount of drag per pass, was periodically adjusted through the use of propulsive aerobrake maneuvers performed at apoapsis. Lower drag pass altitudes can produce more delta-V (velocity), but thermal heating and orbital lifetime constraints limited the allowable drag.

Odyssey was designed as an aerobraking spacecraft, which means that the nominal aerodynamics in the drag configuration are stable. However, the stability characteristics do not necessarily extend to other spacecraft configurations designed to communicate and collect power. A tumbling analysis was performed for various potential safe-mode configurations, which is presented in more detail later in this paper. Although other configurations could have provided superior communications and power characteristics, analysis shows that configurations with the solar array unstowed posed a significant spacecraft tumbling risk. Furthermore, it was determined that the as-built power and thermal systems had enough capability to support the stowed solar-array configuration during safe mode. As a result, the nominal aerobraking configuration shown in Fig. 1 was also chosen to be the safing configuration for Odyssey aerobraking.

The aerobraking process relies upon accurately predicting the timing and duration of drag passes, especially as the orbits become smaller and the ground has less time to respond. Ground-developed sequences, derived from navigation updates, command the spacecraft to be in the proper attitude and configuration for each drag pass. Because the Odyssey aerobraking configuration in the drag-pass attitude did not provide power collection, the allowable time in this attitude was limited. On the other hand, aerodynamic torques observed near periapsis would overwhelm any attempt to control to attitudes other than the aerodynamically stable drag-pass attitude (e.g., to an Earth-point communications attitude). This concern was particularly true for attitude control on the reaction wheels because of the low control authority available. Therefore, a slew to the drag-pass attitude had to be completed before encountering atmospheric drag, and a slew back to Earth point had to occur after completing the drag pass. Some tolerance to sequence timing errors was built into the Odyssey's sequence design. However, sequence timing errors greater than 5 min would generally cause a safe mode entry during the drag pass.

Odyssey's aerobraking sequences were designed to support at least two orbits early in aerobraking and up to nine orbits later in aerobraking when the orbit periods became small. Because these sequences were built well in advance of their use on the spacecraft, aerobraking variabilities adversely affected their timing accuracy. In case of difficulties either deriving or uplinking a new sequence, Odyssey had two ways to modify an existing sequence to correct for timing errors. The ground-based "Jack" contingency procedure and the onboard periapsis timing estimator (PTE) are described, as well as their usage and decision criteria.

Of course, the final safety net for aerobraking was to raise the periapsis out of the atmosphere, thereby eliminating the risk of spacecraft damage by going through a drag pass in an unsafe configuration. Because the so-called pop-up maneuvers must raise the periapsis altitude significantly to get out of the atmosphere ($\sim$50 km, depending upon the periapsis altitude), they consume a considerable amount of fuel. Additional maneuvers would be required to lower the periapsis altitude before resumption of aerobraking. Because of these factors, pop-up maneuvers were clearly undesirable except in case of a obvious emergency. We describe Odyssey's decision criteria for performing an autonomous pop-up (invoked by spacecraft software) and a manual pop-up (commanded by the ground).

Odyssey Aerodynamics Analysis and Modeling

The aerodynamic database for the Mars 2001 Odyssey Orbiter aerobraking was defined using two flow analysis codes: DACFREE, for free molecular flow regime aerophysics simulations, and direct simulation Monte Carlo analysis code (DAC) to perform refined real-gas rarefied flow regime aerophysics simulations. Initial analyses were carried out by using the DACFREE code of Wilmoth,[6] a free-molecular flow analysis code that applies standard free-molecular methods[7] to obtain surface pressure and shear forces, which then can be integrated to obtain aerodynamic forces and moments. Comparison of the results provided good agreement with FREEMAC, the free-molecular code used to develop the Magellan and MGS aerobraking models, which were validated with flight data.

Real-gas analyses were performed by using the DAC code of LeBeau and Wilmoth et al.,[8,9] which applies direct simulation Monte Carlo (DSMC) techniques of Bird[7] for modeling interacting particles in rarefied gas flows. The calculations were all made with an updated version of the Mars atmosphere reacting chemistry model of Hash and Hassan[10] consisting of eight species (O_2, N_2, O, N, NO, C, CO, and CO_2) while accounting for 40 dissociation and 14 exchange reactions. Gas-surface interaction was assumed to be diffuse, noncatalytic, and with full thermal accommodation to a constant specified surface temperature. The DAC code employs a Cartesian grid discretization scheme with embedded Cartesian refinement.[9] The DAC code has been used previously to predict aerodynamics for other Mars-bound spacecraft, including Mars Pathfinder,[11,12] Mars microprobes,[12] and Mars Global Surveyor.[13]

Both DAC and DACFREE codes allow arbitrary surface geometries to be specified as an unstructured collection of triangles. The spacecraft outer surface was defined using the grid-generation code GRIDGEN of Pointwise, Inc., a general purpose software system for generation of three-dimensional grids.[14] The surface definition was transferred directly from a CAD design file via neutral format IGES files. The model includes 30,000+ triangles representing all elements that define the outer surface including the propulsion module, equipment module, thermal blankets, solar arrays, high-gain antenna, solid-state power-amplifier, assembly, propellant tanks, all science deck instruments, battery, launch adapter, launch umbilical towers, engine bell, and shield.

For all configurations analyzed, free molecular calculations were performed using DACFREE. A full sweep of spacecraft attitudes was performed. An Euler sequence convention was used to parameterize Odyssey's aerodynamic force and moment database, where ϕ is the first rotation (about $+Z$) and θ is the second rotation (about $+X$). The aerodynamics vary significantly as the spacecraft goes through a drag pass, with a denser atmosphere experienced at lower altitude. To assess the aerodynamics in this transitional regime, high-fidelity DSMC analyses (with the DAC code) were performed at various trajectory points. The trajectory conditions ranged from the free molecular limit to periapsis flow conditions, which is the location of peak dynamic pressure and peak heating.

The aerodynamic moment coefficients for the nominal aerobraking configuration are shown in Fig. 2. For a given c.g. location, the stable trim angle in pitch is defined by the location at which a negative slope of θ vs C_{MX} crosses the X axis, representing an attitude with zero aerodynamic torque. This characteristic is observed at -0.2 deg for the start of aerobraking, and 2.1 deg for the end of aerobraking (in this notation positive pitch is pitch down, a right-hand rotation about $+X$). The c.g. change between start and end of aerobraking is the result of propellant consumption. As fuel is consumed during the three months of aerobraking, the c.g. migrates

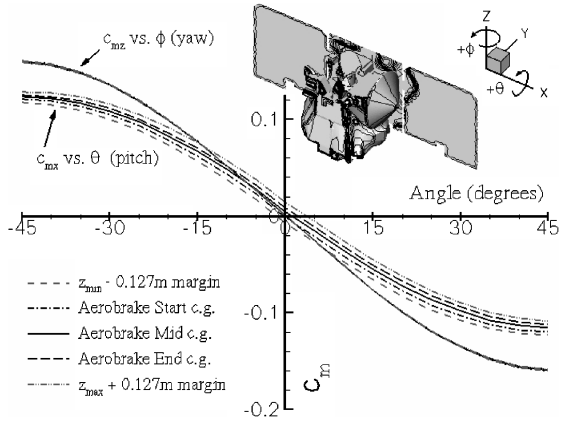

Fig. 2 Mars Odyssey aerobraking free molecular moment coefficients ($A_{ref} = 11.03$ m^2, $L_{ref} = 4.74$ m).

in the positive Z direction. For yaw, the ϕ vs C_{MZ} plot shows the stable trim angle (side slip) is 0.2 deg (positive yaw is a right-hand rotation about $+Z$).

A number of possible safing configurations were analyzed for Odyssey. A free-molecular analysis of one of these configurations is shown in Fig. 3. In this configuration, the solar array is unstowed to increase power available during the vacuum phase of the aerobraking orbit and to minimize the drag area during a drag pass (thereby increasing orbital lifetime). As can be seen in the figure, this configuration has a statically stable trim point at $\phi = -4$ deg (yaw) and $\theta = 27$ deg (pitch) with what appears to be strong pitch and yaw stability margins in the spacecraft body reference frame. However, because of asymmetry about the pitch (Y–Z) plane, conventional theory is not sufficient to assess stability. Taking the same analysis results about a new reference frame aligned with the solar array (by rotating 48 deg about the Y axis, so that the new X axis is aligned with the feathered solar array), it can be shown that there is very little stability margin in the moment normal to the array. This is discussed further in the next section, which shows this configuration to exhibit a high risk of tumbling and a correspondingly high risk of dangerously high vehicle body rates.

Odyssey Tumbling Analysis

As discussed in the preceding section, the nominal aerobraking configuration was designed to be stable during a drag pass. However, off-nominal or safing events could cause the spacecraft to encounter the atmosphere in a different attitude and/or with a different solar-array configuration (e.g., Earth-point configuration rather than the nadir-tracking drag-pass configuration). The robustness of the Odyssey spacecraft to survive such an encounter was analyzed in detail. Although designed as an aerobraking spacecraft, Odyssey has vulnerabilities to certain adverse dynamics and environmental conditions. For example, the harmonic drive actuators used in the solar-array gimbal design can be backdriven with tumbling rates as low as 6 rpm (36 deg/s). Excessive heating of sensitive components, such as thermal louvers, could also occur if the parts of the spacecraft were exposed to the aerodynamic flow. Combined with the tumbling analysis results presented here, these considerations forced a reconfiguration of safe mode.

The original safe-mode configuration is shown in Fig. 3, with the solar array "feathered" to reduce drag in the atmosphere and rotated about the inner gimbal (aligned with the spacecraft Y axis) to increase power collection during the orbit's vacuum phase. As discussed earlier, this configuration is statically stable in the drag pass, as long as the $-Y$ side of the spacecraft faces into the aerodynamic flow.

An analysis was performed to determine the stability of this configuration with off-nominal attitudes. For example, does the attitude stabilize if the solar array initially faces into the aerodynamic flow, or does the spacecraft tumble out of control? An orbital simulation was created to answer this question. The simulation includes

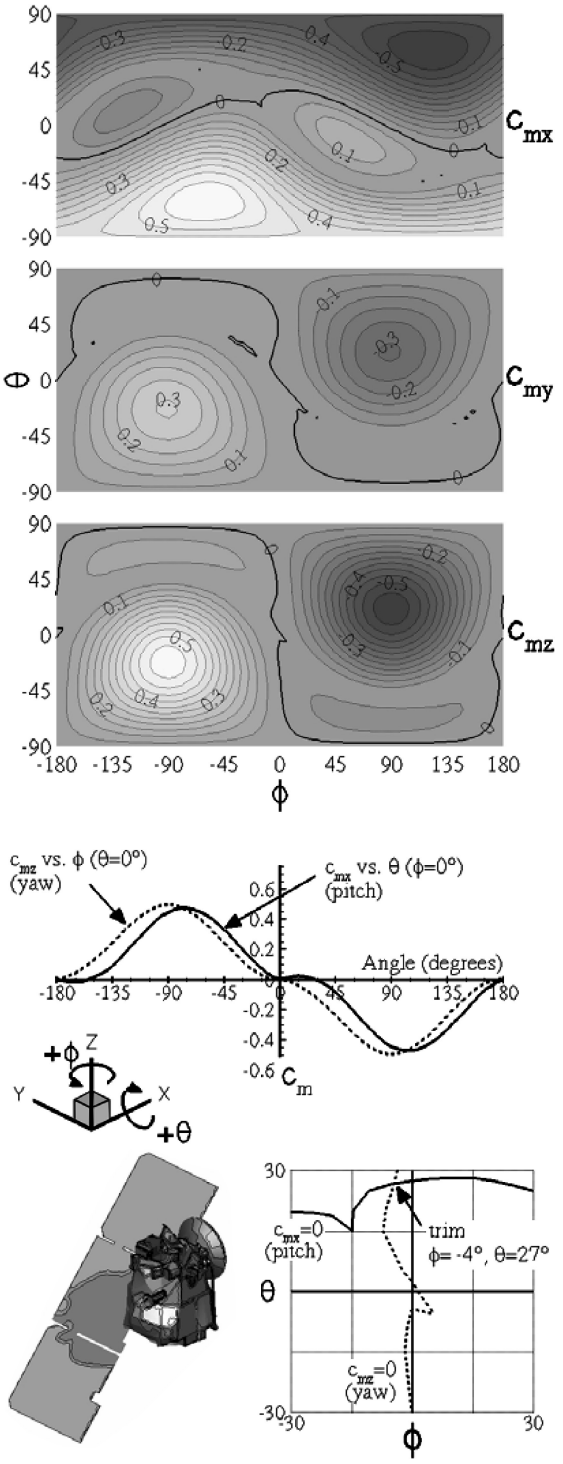

Fig. 3 Mars Odyssey feathered array (inner gimbal = −48 deg, outer gimbal = 0 deg) free-molecular moment coefficients ($A_{ref} = 11.03$ m^2, $L_{ref} = 4.74$ m).

Odyssey's aerodynamic database [force and moment coefficients from the computational-fluid-dynamics (CFD) results discussed earlier] and a simple atmospheric model derived from Mars-GRAM 2000.[15] The simulation was initialized assuming inertial hold on reaction wheels, and the entire range of possible encounter attitudes was surveyed. The normal safing responses were assumed active, such that thruster-based rate damping control was commanded when excessive attitude or rate errors were observed. The results of this simulation are shown in Figs. 4 and 5.

In Fig. 4, the cases where uncontrollable tumbling occurred are shown in light gray on the "stability sphere" on the left, and the configuration of the spacecraft (including the spacecraft coordinate

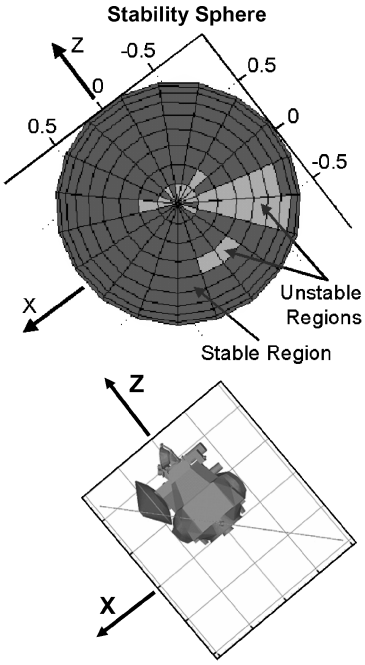

Fig. 4 Tumbling characteristics of original safe-mode configuration.

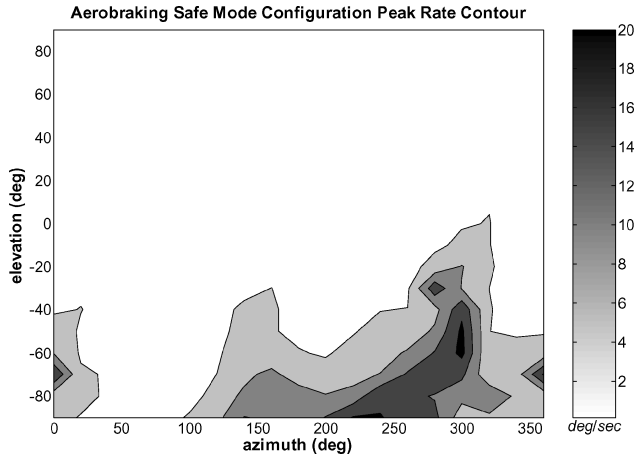

Fig. 5 Tumbling rates vary with geometry of atmospheric encounter.

frame) is shown on the right. The stability sphere shows tumbling conditions as a function of the spacecraft axis initially aligned with the velocity vector. The rate threshold for defining uncontrollable tumbling is 15 deg/s. As shown, the origin of the plot represents the $+Y$ axis aligned with the velocity vector, that is, the $+Y$ axis is pointed into the aerodynamic flow. The grid outward from the origin is spaced equally with 10-deg increments. The plot does satisfy our intuition, in that tumbling conditions would likely occur with the solar array leading the spacecraft into the atmosphere. (The other side of the sphere shows no uncontrollable tumbling with the solar array trailing the spacecraft, and so is not presented here.)

More detail of the tumbling characteristics are shown in Fig. 5 for this configuration, where the tumbling rates are shown as a function of the initial aerodynamic flow direction. Tumbling rates are shown as functions of aerodynamic flow azimuth (Az) and elevation (El) relative to the $-Z$ axis of the spacecraft. That is, the $-Z$ axis is aligned with the velocity vector for $Az = 0$ and $El = 0$, implying that the $-Z$ face of the spacecraft is facing into the aerodynamic flow. The azimuth is defined as a positive rotation about the spacecraft Y axis, so that for $Az = 90$ deg and $El = 0$ the $+X$ face of the spacecraft faces into the aerodynamic flow. Similarly, elevation is defined as a positive rotation about the spacecraft X axis, so that for $Az = 0$ and $El = -90$ deg the $+Y$ face of the spacecraft faces into

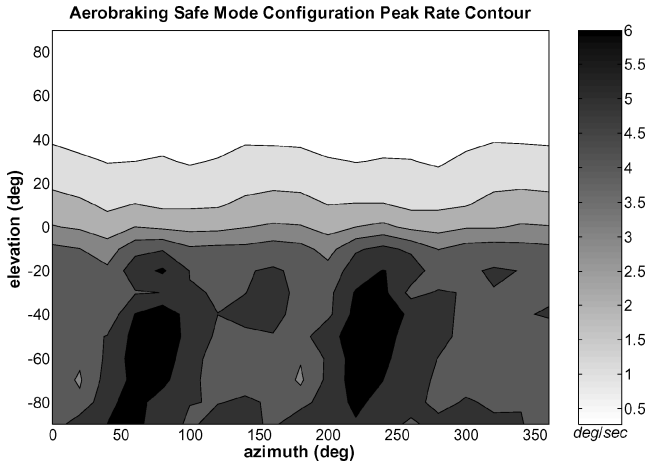

Fig. 6 Improved tumbling characteristics of revised safe-mode configuration.

the flow. As can be seen in Fig. 5, orientations with azimuth angles around 300 deg, and with negative elevation angles, have the highest likelihood of uncontrolled tumbling. Negative elevation angles correspond to the solar array leading the spacecraft into the drag pass. Tumbling rates exceed 20 deg/s in the worst-case initial orientations. Because of the high risk of spacecraft damage with such high tumbling rates and because there is no guarantee that the spacecraft could not be in such an attitude just before the drag pass (e.g., in the case of sun search maneuvers resulting from loss of attitude knowledge), this safing configuration was considered unacceptable.

A number of alternative safe-mode configurations were considered. A careful review of the power budgets and the communications link margins revealed that the nominal drag configuration shown in Fig. 1 could also be used as the safing configuration. With the solar array stowed, it was theorized that this configuration would be much less likely to tumble. As seen in Fig. 6, the highest rates remain less than 6 deg/s with the stowed solar-array configuration, compared with rates of more than 20 deg/s with the solar array feathered. The smaller rates shown pose no risk of damage to the spacecraft. The only drawback to this configuration is the larger amount of drag. In safe mode, the smallest drag possible is desired, thereby increasing orbital life and giving the ground more time to respond to a safing event. Although the shorter orbital life was a significant concern, implementation of an autonomous pop-up maneuver for aerobraking's final phase mitigated the issue and allowed the nominal drag-pass configuration to be adopted as the safe-mode configuration as well. The autonomous pop-up will be discussed in more detail later in this paper.

Nominal Drag-Pass Sequencing

All drag-pass sequences uplinked to the spacecraft were built using predicted periapsis times. After each drag pass, the navigation team computed an orbit determination solution by using radiometric data from the spacecraft along with the Mars-GRAM 2000 atmospheric model in the navigation software. These solutions both predict the periapsis times and expected drag durations for subsequent orbits, as well as reconstruct the periapsis times and drag magnitudes of previous orbits. The navigation team was given a requirement to predict the time of periapsis passage to within 5 min. The sequence design was heavily dependent on navigation's ability to meet this requirement. Five-minute timing margins, called "guard bands," were included in the sequence to ensure the proper spacecraft attitude and configuration for the drag pass. If the timing requirement were to be violated, the spacecraft would not be in the proper configuration for the drag pass, likely resulting in safe-mode entry.

As the orbit periods became shorter, the ground team could not turn around new sequence builds for every orbit. The navigation team was required to provide accurate solutions for more orbits into the future. The length of time the sequence build was valid depended entirely on how far ahead navigation could predict the

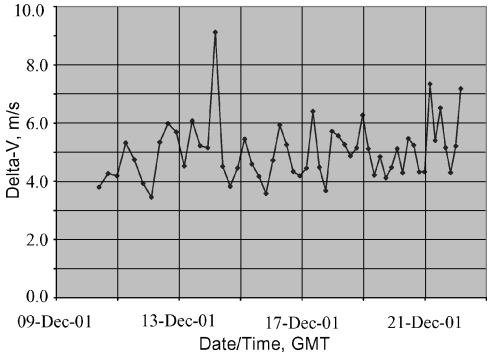

Fig. 7 Variability of the Mars atmosphere measured by drag-pass delta-V.

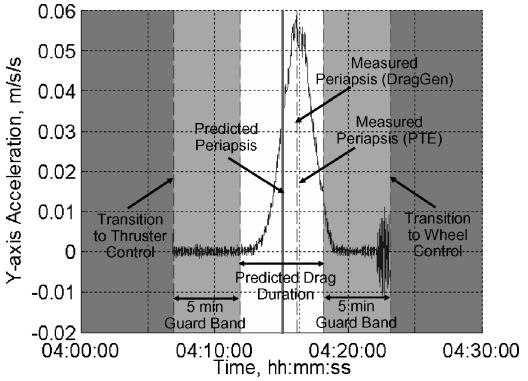

Fig. 8 Orbit 106 "monster" drag pass.

time of periapsis passage to within 5 min. In the larger orbit periods, navigation could only predict one or two orbits ahead. For orbit periods less than 3 h, navigation was able to predict ahead more than 10 orbits. From an operations perspective, it was desirable to include as many orbits into each sequence as possible, thereby reducing the number of sequence builds. However, the further out navigation predicted, the greater the chance that atmospheric variability would produce timing errors in excess of the 5-min limit.

The limiting factor in predicting future periapsis times was the high variability of the Mars atmosphere. Figure 7 shows drag magnitudes for the period of time Odyssey was aerobraking over the north pole. Based on MGS aerobraking data, the Mars atmosphere was expected to have the least variability in the polar regions. Odyssey aerobraking did confirm this expectation, and Odyssey took advantage of the lower variability by reducing the periapsis altitude and increasing the amount of drag per pass. However, the variability was still quite significant as shown in Fig. 7. Even though the peripsis altitude varied by less than 3 km over this time period, the drag magnitude varied by nearly 300% from the highest pass to the lowest pass. Because of fundamental limits on how much heating the spacecraft can handle, this variability restricts how aggressively the aerobraking operations can be flown. Furthermore, the variability of delta-V from one drag pass to the next limits how accurately the Navigation team can predict the timing of future orbits.

Data from two subsequent drag passes will be used to illustrate the impact of atmospheric variability on sequence timing and the potential threat to vehicle safety. Figure 8 shows the largest drag pass that Odyssey experienced, which occurred on orbit 106 during the "quiet period" over the north pole. (This drag pass corresponds to the highest peak in Fig. 7.) Figure 8 shows the acceleration on the vehicle as a function of time as measured by the inertial measurement unit's accelerometers. The peak acceleration, the peak heating (as measured by thermocouples on the solar array), and the drag-pass delta-V were all more than 100% higher than predicted by the orbit determination solution. The orbit determination solution also predicted that the periapsis would happen slightly earlier than it did, by approximately 66 s. Two measurements of the actual periapsis time are shown; one is computed onboard by the PTE algorithm,

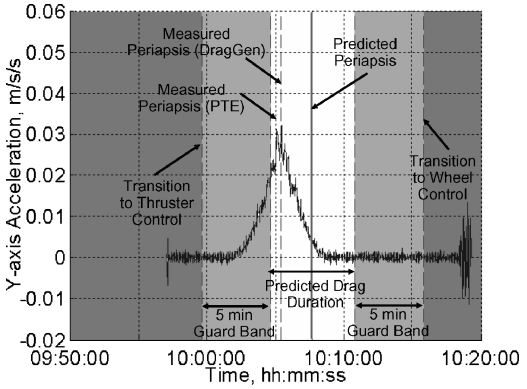

Fig. 9 Orbit 107 nominal drag pass.

which will be discussed in more detail later, and the other is computed from flight telemetry by a piece of ground software called DragGen. Both methods use accelerometer data in computing the periapsis time. The expected drag duration is also shown on the plot, along with the 5-min guard bands on either side of the drag pass. Prior the drag pass, the spacecraft transitions from reaction-wheel control to thruster control, and following the drag pass the spacecraft transitions from thruster control back to wheel control. Because of the low control authority of the reaction wheels, loss of attitude control would result if the acceleration "tails" were to creep past either guard band. The 66-s timing error on orbit 106 still leaves nearly 4 min of margin in the guard bands.

Figure 9 shows the subsequent drag pass for orbit 107, which occurred less than 6 h following the huge drag pass experienced on orbit 106. The drag magnitude on this pass was within a few percent of the orbit determination prediction. At this time in the mission, the navigation team was predicting two orbits at a time, so that both drag passes were predicted using the same navigation data. As can be seen by comparing Fig. 9 to Fig. 8, the large drag pass of orbit 106 shifted the timing dramatically. Whereas the periapsis time on orbit 106 was 66 s later than predicted, the orbit 107 periapsis time was 141 s early. Because of the much larger than expected delta-V on orbit 106, there was a timing shift between the two orbits of 207 s. Fortunately, the timing on orbit 106 was 66 s later than predicted. Had the timing for orbit 106 been 100 s early instead, the timing shift between the two orbits would have placed the acceleration tails of orbit 107 past the reaction-wheel transition point. If left uncorrected, this would have led to a loss of attitude control and subsequent safe-mode entry. Although "safe" for the spacecraft health, safe-mode orbits consume more fuel and delay the aerobraking timeline. Because of this concern, two tools were developed to correct for timing errors like this. These tools allowed the operations team to use drag-pass results from one orbit to correct timing for the next orbit without generating a new orbit determination solution. These tools will be described in the next section.

"Jack" Contingency Procedure

To correct for large timing errors (those in excess of 5 min), the ground operations team had a contingency plan to manually adjust the timing of a running onboard sequence. For historical reasons not entirely clear, this procedure is known as the Jack procedure. For large orbital periods, the procedure was not required because there was sufficient time for the navigation team to provide an updated orbit determination solution every orbit, and for the operations team to build and uplink a new sequence. When the orbit period dropped below 6 h, the nominal sequence build process (based on navigation orbit reconstruction) could not safely generate an updated sequence and uplink it in time for the next drag pass. Here the Jack procedure could then come into play.

After every drag pass, the operations team would compute the actual periapsis time from spacecraft telemetry, primarily based on spacecraft accelerometer data. The operations team would also compute how close the drag delta-V was to navigation predictions. These two pieces of information were used in ground software to predict

where the next drag-pass periapsis would be and what the timing error would be relative to the navigation predict. Predicted timing errors in excess of 5 min for the next orbit triggered the Jack contingency procedure. The procedure resulted in the ground uploading a timing bias parameter, utilized by the sequence to shift the timing of the commands by the appropriate amount to keep the sequence approximately centered about periapsis. A demonstration of the Jack procedure was executed once on Odyssey just before the orbit period reached 6 h. However, the Jack procedure was never required for actual flight operations. Although there were sequences in flight that would have violated the 5-min requirement if left uncorrected, the onboard PTE algorithm performed the timing adjustment rather than the ground-based Jack procedure. The PTE algorithm is described in the next section.

PTE Algorithm

The PTE software is very similar to the Jack contingency procedure in that it can shift a command sequence in time. However, it differs in two important respects. First, PTE is part of the onboard flight software. Once configured and activated, PTE operates autonomously. It provides sequence adjustments even if the ground operations team was unable to do so. Second, PTE is a reactive process; it shifts the upcoming orbit event sequence based solely on the timing error detected during the last drag pass. Whereas the Jack contingency procedure also looks at differences between the observed delta-V magnitude and the predicted delta-V magnitude, PTE was simplified to operate onboard the spacecraft and has no predictive capabilities. PTE only compares the observed periapsis time to the predicted periapsis time. As a result, the PTE timing correction tends to lag by one orbit. This makes the PTE software effective in tracking and correcting timing error trends, but less effective in accommodating statistical fluctuations.

The PTE software computes its estimate of timing error by examining the accelerometer data throughout the drag pass. PTE uses a centroiding scheme to find the "center" of the acceleration curve (see Figs. 8 and 9). PTE's estimate of periapsis time is compared to the navigation prediction of periapsis time, and the error is computed as the difference between the two. If enabled, the resultant timing error is used to shift the execution of all subsequent drag-pass sequences.

Although the reactive nature of the PTE software might appear to be limiting, it is only an issue for the large orbit periods at the start of aerobraking. In these large period orbits, small variations in drag-pass delta-V result in large changes in orbit period and correspondingly large changes in periapsis timing. However, the operations team generated a new Odyssey command sequence for every orbit when the orbit period was larger than 6 h. This approach discovered and corrected timing errors before each new drag pass. Uplink of a new command sequence cleared any adjustments computed by the PTE software. When the orbit period shrank to less than 6 h (more than $\frac{2}{3}$ of the total aerobraking orbits were shorter than this), the period reduction for a given delta-V was small enough that the inherent PTE lag was acceptable. PTE's usefulness became more apparent with these shorter orbits.

Operationally, PTE was running during every Odyssey drag pass, although it was prevented from commanding a sequence shift until the operations team became comfortable with its performance. PTE would not have had an effect early on because new command sequences were built and uplinked for each orbit, thereby overwriting any PTE correction. Once multiple orbit sequences were used, the performance of PTE was found to be very good. Only for a handful of medium-sized orbits did PTE command a time shift that increased the timing error of a future drag pass rather than decreasing it. This was caused by PTE's inability to account for large delta-V variations from the navigation predict. For example, a larger-than-expected delta-V tends to counteract a late periapsis time; the next uncorrected periapsis time can actually be early compared with predicts if the delta-V variation were large enough. This effect diminishes in smaller orbits because the nominal orbit period change per drag pass becomes far less. Once the orbit period was less than about 5 h, PTE managed the periapsis timing error to less than 90 s in most cases, and comfortably less than the 5-min guard-band limit in all cases. The sequences over this period started with three orbits in each build and ranged up to six orbits in each build at the end of aerobraking. The residual PTE timing errors for all of Odyssey aerobraking are shown in Fig. 10.

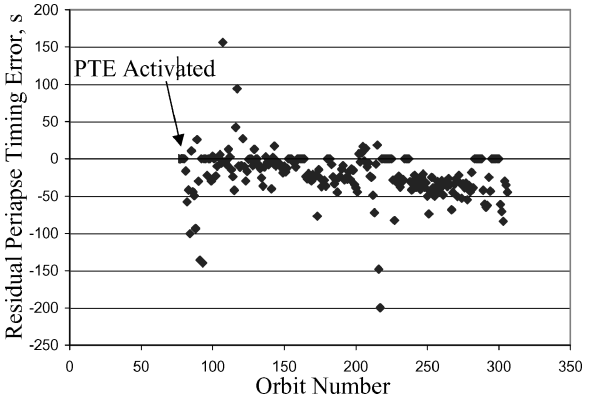

Fig. 10 Periapsis timing estimator timing corrections.

Pop-Up Maneuvers

As the name implies, the pop-up maneuver is designed to raise the periapsis altitude out of the atmosphere. For Odyssey, pop-up burns were to be used only in the event of serious spacecraft anomalies. The pop-up burn magnitudes were sized to provide a periapsis altitude at which the spacecraft could safely remain Earth pointed using reaction-wheel control. The periapsis altitude targeted was approximately 155 km. A pop-up maneuver would preclude resumption of aerobraking until the anomaly was resolved.

Two types of pop-up maneuvers were defined for Odyssey aerobraking operations. The first type was built as a ground-commanded (manual) pop-up burn. The design was similar to the corridor control maneuvers used to maintain the aerobraking periapsis altitude, although the pop-up burn magnitude was much larger than the other burns. As aerobraking progressed, the orbit period decreased, and the apoapsis altitude became lower, making the pop-up maneuver less efficient. The magnitude had to be adjusted each week to provide the required periapsis altitude.

In addition to the ground commanded pop-up maneuver, the spacecraft had the capability to perform an autonomous pop-up burn. This capability was desired for late aerobraking operations as the orbit periapsis moved southward from the north pole of Mars. The oblateness of Mars, coupled with the periapsis precession, created the tendency for the spacecraft to be pulled deeper into the atmosphere during this phase. This tendency was nominally counteracted by ground commanded periapsis raise maneuvers. By the last week of aerobraking, "up" maneuvers were required every day to maintain a 24-h margin against burning up in the Mars atmosphere. Because of the potential mission-ending risk, the autonomous pop-up maneuver was enabled during the period where periapsis precessed southward. In the event of a spacecraft safe-mode entry, the pop-up maneuver was designed to execute at the next apoapsis. The burn was triggered by using a burn-time table, which was updated with every drag-pass sequence build based on the latest navigation orbit predictions. Like the manual pop-up maneuver magnitude, the autonomous pop-up maneuver magnitude was resized weekly to provide a safe periapsis altitude.

The autonomous pop-up maneuver ensured that a safe-mode entry caused by onboard fault protection would immediately suspend aerobraking and keep the spacecraft safe. The autonomous pop-up maneuver was also utilized as a safety net in case a new sequence could not be uplinked to the spacecraft. To mitigate concerns of a deep-space-network tracking station problem preventing uplink of a new sequence, each drag sequence build contained a safe-mode entry after the last orbit in the sequence. Thus a failure to uplink a new sequence would result in the currently executing sequence timing out and issuing the safe-mode entry command. An autonomous pop-up burn would execute at the subsequent apoapsis.

Fortunately, there were no serious anomalies on Odyssey requiring either an autonomous or manual pop-up maneuver. Odyssey did have one software-related safe-mode entry early in aerobraking (on orbit 5), but the atmospheric drag was small at that point, and no burns were necessary to safe the spacecraft.

Conclusions

In this paper, we have presented an overview of the flight software, ground software, and operational approaches that kept Odyssey aerodynamically safe during aerobraking and limited the risks to the vehicle during this inherently hazardous operational phase. The design served the vehicle well. Early detailed design and analysis work established a safe, tumble-free configuration for safing Odyssey. The operational constraints placed on the sequence timing and navigation accuracy were well understood and were maintained throughout aerobraking. Although no serious anomalies occurred during Odyssey's aerobraking mission phase that might have required drastic responses, such as safe-mode entry and manual or autonomous pop-up maneuvers, the design was in place to prevent jeopardizing the mission in case they were needed. Other features described in this paper, especially the periapsis-time-estimation algorithm, were routinely used during aerobraking and proved very effective. The success of Odyssey's aerobraking demonstrates that the risks of aerobraking can be effectively managed and has thereby expanded the aerobraking technology base for future interplanetary spacecraft.

Acknowledgments

This work was supported by the Mars Surveyor Program 2001, under contract to the Jet Propulsion Laboratory, Contract 961162. Many thanks go to the dedicated engineers at Lockheed Martin who developed the Odyssey aerobraking safing design, worked through the details, and made it flight-worthy. Special acknowledgment is given to Larry Adams, who led the special study for aerobraking safing; Guy Beutelschies, who developed the fault-tree analysis and worst-case timing estimates; and Eric Seale and Jason Dates, who architected the Odyssey flight software for safing.

References

[1]"Mars Surveyor 2001 Mission Plan," Rev. B, Jet Propulsion Lab., JPL D-16303, Pasadena, CA, Aug. 2000.

[2]Lyons, D. T., Saunders, R. S., and Griffith, D. G., "The Magellan Venus Mapping Mission: Aerobraking Operations," International Astronautical Federation, Oct. 1993.

[3]Spath, S. R., and Eckart, D. F., "Fuel Optimization During Mars Global Surveyor Aerobraking," AAS Paper 2000-072, Feb. 2000.

[4]Oberg, J., "Why the Mars Probe Went Off Course," *IEEE Spectrum*, Vol. 36, No. 12, 1999.

[5]Euler, E. A., Jolly, S. D., and Curtis, H. H., "The Failures of the Mars Climate Orbiter and Mars Polar Lander: A Perspective from the People Involved," AAS Paper 2001-074, Feb. 2001.

[6]Wilmoth, R. G., *DACFREE—A Free-Molecular/Newtonian Code for Hypersonic Flow, A Users Guide*, 1999.

[7]Bird, G. A., *Molecular Gas Dynamics and the Direct Simulation of Gas Flows*, Clarendon, Oxford, 1994.

[8]LeBeau, G. J., "A User Guide for the DSMC Analysis Code (DAC) Software for Simulating Rarefied Gas Dynamics Environments," Rev. DAC97-G, NASA, Jan. 2002.

[9]Wilmoth, R. G., LeBeau, G. J., and Carlson, A. B., "DSMC Grid Methodologies for Computing Low-Density Hypersonic Flows About Reusable Launch Vehicles," AIAA Paper 96-1812, June 1996.

[10]Hash, D. B., and Hassan, H. A., "Monte Carlo Simulation of Entry in the Martian Atmosphere," *Journal of Thermophysics and Heat Transfer*, Vol. 7, No. 2, 1993, pp. 228–232.

[11]Moss, J. N., Blanchard, R. C., Wilmoth, R. G., and Braun, R. D., "Mars Pathfinder Rarefied Aerodynamics: Computations and Measurements," AIAA Paper 98-0298, Jan. 1998.

[12]Moss, J. N., Wilmoth, R. G., and Price, J. M., "DSMC Simulations of Blunt Body Flows for Mars Entries: Mars Pathfinder and Mars Microprobe Capsules," AIAA Paper 97-2508, June 1997.

[13]Wilmoth, R. G., Rault, D. F., Cheatwood, F. M., Engelund, W. C., and Shane, R. W., "Rarefied Aerothermodynamic Predictions for Mars Global Surveyor," *Journal of Spacecraft and Rockets*, Vol. 36, No. 3, 1999, pp. 314–322.

[14]*GRIDGEN User Manual*, Pointwise, Inc., 1999.

[15]Justus, C. G., and James, B. F., "Mars Global Reference Atmospheric Model, 2000 Version (Mars-GRAM 2000): Users Guide," NASA TM-2000-210279, May 2000.

R. Mase
Guest Editor